Large Synoptic Survey Telescope

www.lsst.org

LSST Astrometry: Simulations and Numerical Studies

Željko Ivezić[1], D. Monet[2], A. Connolly[1], S. Krughoff[1], A. Walker[3]

[1]University of Washington, [2]U. S. Naval Observatory Flagstaff Station, [3]Cerro Tololo Inter-American Observatory

Astrometry is an important part of the Large Synoptic Survey Telescope (LSST; http://lsst.org) program. This is reflected in the requirement in the Science Requirements Document for a maximum of 10mas differential astrometric error from a single measure of a star with high signal-to-noise ratio. Assuming that this requirement will be met, the LSST will obtain parallax and proper-motion measurements of comparable accuracy to those of Gaia at its faint limit (r<20) and smoothly extend the error versus magnitude curve deeper by about 5 mag. Recent efforts to reduce the risk for this requirement have concentrated in two areas. First, the LSST Image Simulator has been used to generate sequences of images containing stars with various astrometric parameters and a range of simulated observing conditions. Second, short exposure observations from data archives have been processed, and new observations have been requested from various telescopes, including the Dark Energy Camera and the Space Surveillance Telescope. Results from these investigations will be presented, and the predictions for the astrometric performance of LSST will be discussed.

1. Numerical Simulations

The LSST Image Simulator (ImSim) has been used to study two key areas of astrometric performance. The first is the astrometric error for a single measure of a single coordinate for a single star. A sequence of 6 steps of elevation (30, 42, 53, 65, 76, 84 degrees) was chosen on a single night, and 143 stars of various magnitudes were simulated in each of 5 bands (g, r, i, z, y). Figure 1 shows the RA (red) and Dec (blue) components of the differential chromatic refraction (DCR), and Figure 2 shows the astrometric error (mas) for the RA (red) and Dec solutions as a function of g-band magnitude. The plateau in error at the faint magnitudes comes from the small sample size.

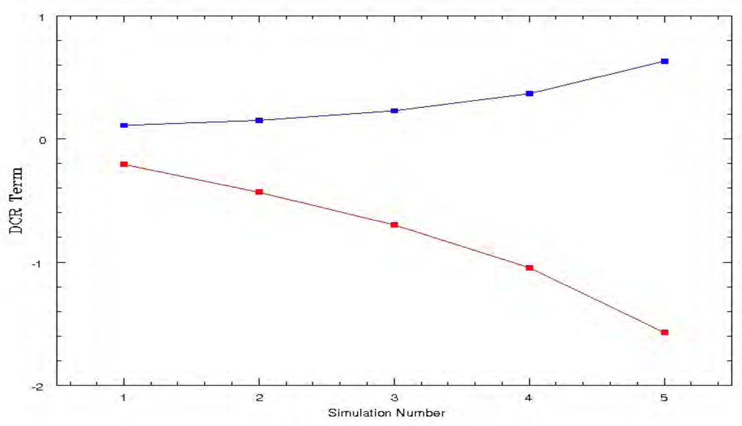

Fig. 1. Differential Chromatic Refraction values in RA (red) and Dec (blue).

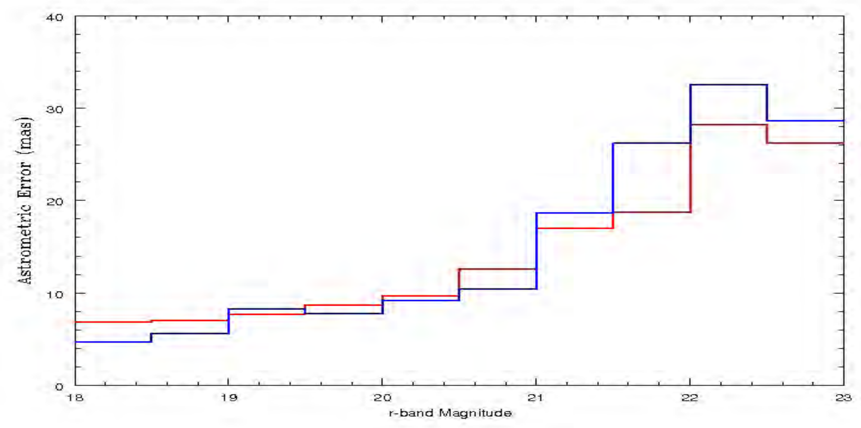

Fig. 2. Growth of astrometric error as a function of magnitude in g-band.

The second area of study was the ability to construct a single astrometric solution that includes all measures from all colors and all zenith distances. The theoretical prediction is that the refractive displacement for each star in each color is a unique coefficient that multiplies the geometric term of ZDX=tan(ZD)sin(PA) in R.A. and ZDY=tan(ZD)cos(PA) in Dec., where ZD is the zenith distance and PA is the parallactic angle at the epoch of the observation. To incorporate multiple filters, the baseline astrometric pipeline algorithm was expanded to include a vector of DCR coefficients while retaining only single terms for position, proper motion, and parallax. Although the exact values for the refractive amplitudes are complicated integrals of the object's spectral energy distribution and the sensitivity of the telescope and camera, a general correlation with broadband color is expected: red stars should refract less than blue stars. Figure 3 shows the results of the single fit for the simulation discussed above.

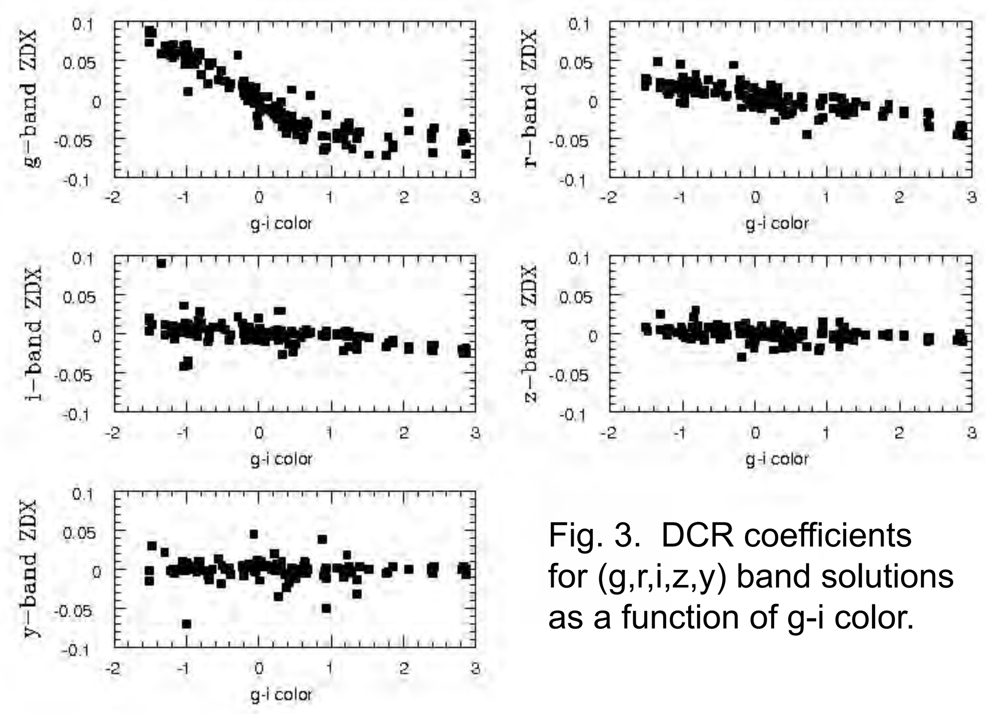

Fig. 3. DCR coefficients for (g,r,i,z,y) band solutions as a function of g-i color.

Another important astrometric study is whether DCR coefficients can be used to identify objects with non-stellar spectra. A simulation of several stars and QSOs was done. The QSO spectral energy distributions were taken from the SDSS DR9[1] server. Figure 4 shows the DCR coefficients computed from (u,g,r,i) simulations. It is obvious that the refraction in u- and g-band is quite different, but this is predicted from the broadband colors. A future study will pursue this concept with stars and QSOs of similar broadband color.

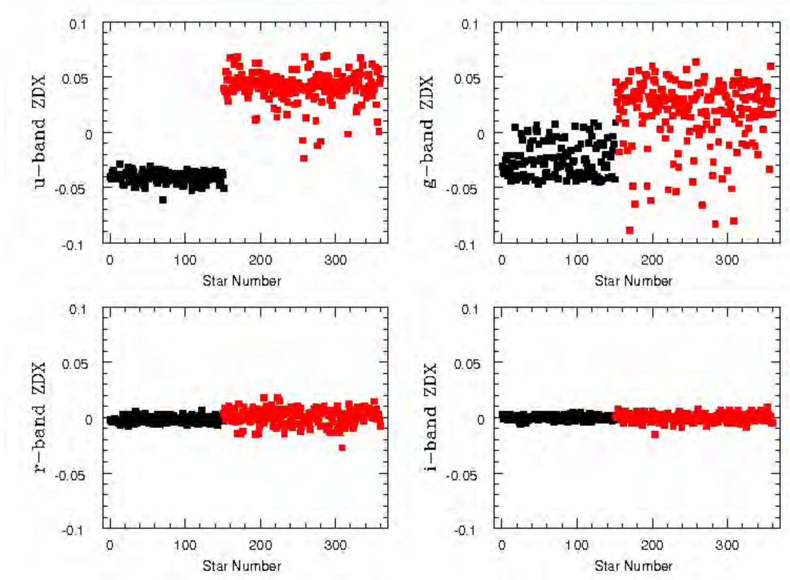

Fig. 4. DCR coefficients for a sample of stars (black) and QSOs (red) in (u,g,r,i).

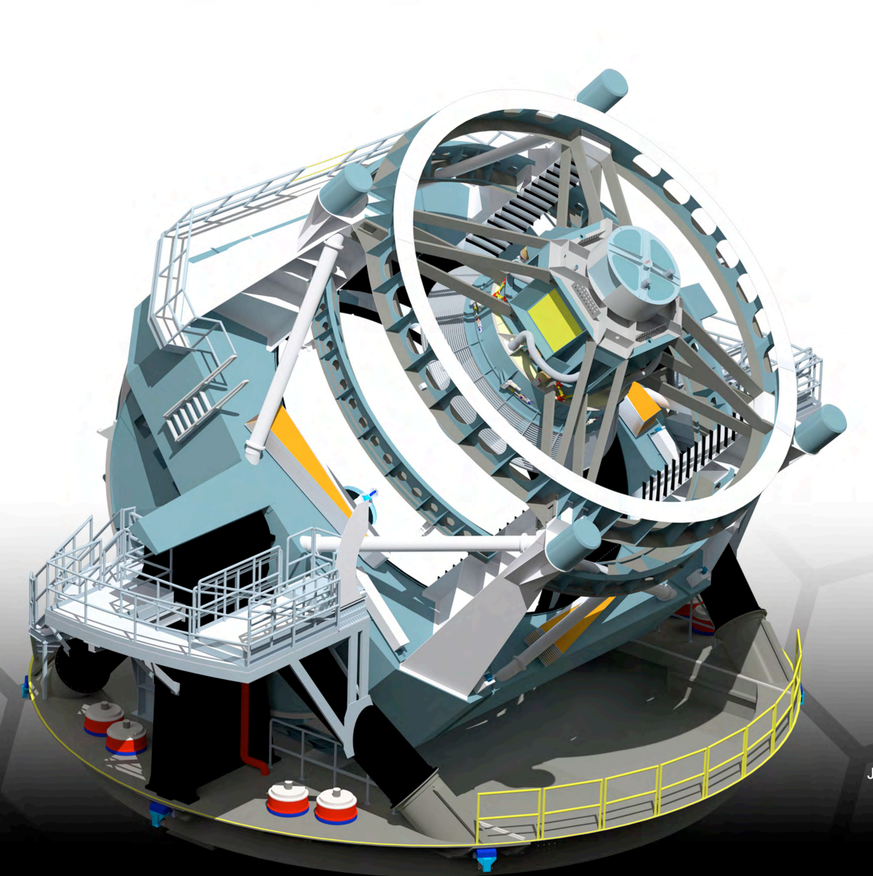

January 2013

2. Short Exposure Observations With the Dark Energy Camera

A legacy of astrometric experience gained at the USNO Flagstaff Station and other sites demonstrates that the astrometric error measured in large field, short exposure images can be dominated by effects arising from seeing. For its parallax program, USNO uses a minimum of 5 minute exposures for a 10 arcminute field of view. LSST's observations will be a pair of 15 second exposures covering 9.6 square degrees. During the preparation of the LSST Science Requirements Document (SRD), astrometric studies of data were taken with a variety of telescopes (Subaru, CTIO 4-m, Gemini South) to provide support for the value presented in the SRD. The recent commissioning of the Dark Energy Camera (DECam) provided a new opportunity to collect wide field, short exposure observations under circumstances remarkably similar to those expected for LSST.

The DECam data were sequences of 5 exposures in each of 4 times (1, 3, 10, 30 seconds) on a field near NGC 288. SExtractor[2] was used to compute centroids for all images in each of the 62 CCDs in the DECam. For each CCD in each exposure, three astrometric fits were done using (constant, linear, cubic) models for the transformation between the individual images and the mean coordinate system. In the mean system, all pairs of stars observed on each CCD were identified, and the mean and standard deviation of the separation between the stars in each pair were computed from the 5 exposures in each sequence. The result is the growth of the astrometric error as a function of the distance between stars as a function of the distance and of the exposure time. Figure 5 shows such a plot for a night of "good" seeing (about 1.2 arcsec FWHM) and Figure 6 for a night of "bad" seeing (about 1.8 arcsec FWHM). In each, the constant solution is shown with triangles, the linear solution with squares, and the cubic solution with circles.

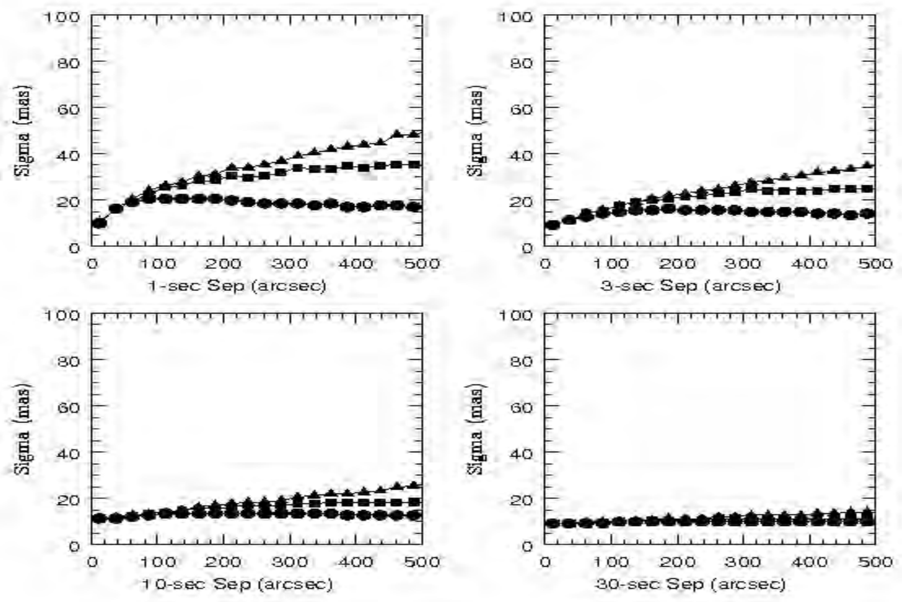

Fig. 5. Growth of astrometric error as a function of separation for a "good" night.

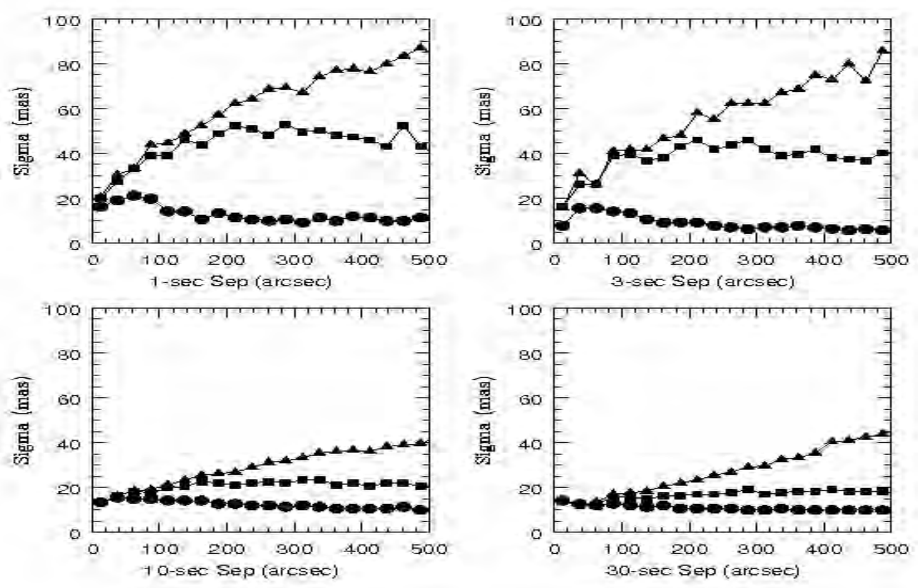

Fig. 6. Growth of astrometric error as a function of separation for a "bad" night.

3. Conclusions and Acknowledgements

The results from the ImSim are encouraging, but the astrometric accuracy seems better than what was expected. In particular, the size of the astrometric error continues to decrease for stars brighter than those included in this sample, and there is little ground-based legacy to support single-measure errors much smaller than about 3mas. More numerical experiments are needed to understand this issue, and changes to the ImSim seeing masks may be needed.

The results from the DECam are quite encouraging. Real data from a real sensor at a comparable site carry large weight, and it is encouraging to see that the quality of the astrometry is correlated with the quality of the night as measured by the image FWHM and the comments of the observers. The astrometric solutions based on only a constant transformation might include an error term arising from the size of the dithers between exposures, and in any case it is unreasonable to adopt such a primitive model for the LSST pipeline. The important result is that on nights of both "good" and "bad" seeing that a cubic transformation provides an adequate model of the residual refractive effects of the atmosphere over the spatial scales needed for a single astrometric solution per LSST CCD. If confirmed by more observations, this can be used to add robustness to the LSST astrometric pipeline processing.

This research makes use of data provided by Cerro Tololo Inter-American Observatory, as distributed by the NOAO Science Archive. NOAO is operated by the Association of Universities for Research in Astronomy (AURA) under cooperative agreement with the National Science Foundation. Observations were taken with DECam, built by FNAL under auspices of the Dark Energy Survey collaboration.

[1]http://dr9.sdss3.org/advancedSearch
[2]http://www.astromatic.net/software/sextractor

LSST is a public-private partnership. Design and development activity is supported in part by the National Science Foundation. Additional funding comes from private gifts, grants to universities, and in-kind support at Department of Energy laboratories and other LSSTC Institutional Members.